JOURNAL OF SOLID STATE CHEMISTRY 78, 84–92 (1989)

Chemically Twinned Phases in the Ag_2S–PbS–Bi_2S_3 System

Part II. Powder X-Ray Diffraction Analysis

A. SKOWRON AND R. J. D. TILLEY

Department of Materials Science and Metallurgical Engineering, University College, Newport Road, Cardiff CF2 1TA, United Kingdom

Received August 8, 1988

Powder X-ray diffraction has been used to study chemically twinned phases occurring in the PbS-rich region of the Ag_2S–PbS–Bi_2S_3 system. Six structures were characterized. A new chemically twinned phase built up of *galena*-like slabs eight octahedra wide has an orthorhombic unit cell with a = 1.3565(4) nm, b = 3.3046(7) nm, c = 0.4102(2) nm, space group *Bbmm*. Vikingite, containing alternating *galena*-like slabs four and seven octahedra wide has a monoclinic unit cell with a = 1.3461(3) nm, b = 2.5664(7) nm, c = 0.4105(1), γ = 95.57(2)°, and *B*2/*m* or *Bm* as space group. The b parameters of the two twinned phases which existed over appreciable composition ranges were found to decrease as the overall composition became richer in Ag while the a and c unit cell parameters did not alter significantly. Reasons for these changes are discussed. © 1989 Academic Press, Inc.

Introduction

The phases of interest in this study of the Ag_2S–PbS–Bi_2S_3 system are based on a common structural principle, called chemical twinning or unit cell twinning, first named by Andersson and Hyde (*1*). In this, twin planes introduced into the crystal matrix serve the purpose of accommodating changes in anion to cation ratio without recourse to other structural defects. Two such phases occur in the PbS–Bi_2S_3 system, the minerals lillianite and heyrovskyite (*2–4*). These and a number of others were found when Ag_2S was added as an additional component to form the Ag_2S–PbS–Bi_2S_3 system (*5–9*).

The idealized structures of two of these phases are shown in Fig. 1. As can be seen, they are formed by stacking parallel slabs of material with the *galena* structure, each slab being in a twinned relationship to its neighbor. The distinction between the phases lies in the widths of *galena*-like slabs. A convenient measure of this width is the number of octahedra running diagonally across the *galena* band, which can also provide a convenient means of labeling the phases. Thus the phases shown in Fig. 1 can be represented as *L*4,7 and *L*8,8, where the symbol *L* indicates that the phases all belong to the same family as lillianite, *L*4,4, which can be regarded as the parent phase of the homologous series. The unit cell parameters of the phases reported to date can be found in Table I.

Silver can play two roles in the formation of lillianite-type phases (*6–10*). In addition to the apparent ability to stabilize a variety of structures which do not form in the parent PbS–Bi_2S_3 system, silver can also be incorporated into the lattice in various amounts to cause a change in unit cell dimensions without changing the number of octahedra in the *galena*-like slabs. This can be illustrated by a consideration of two

0022-4596/89 $3.00

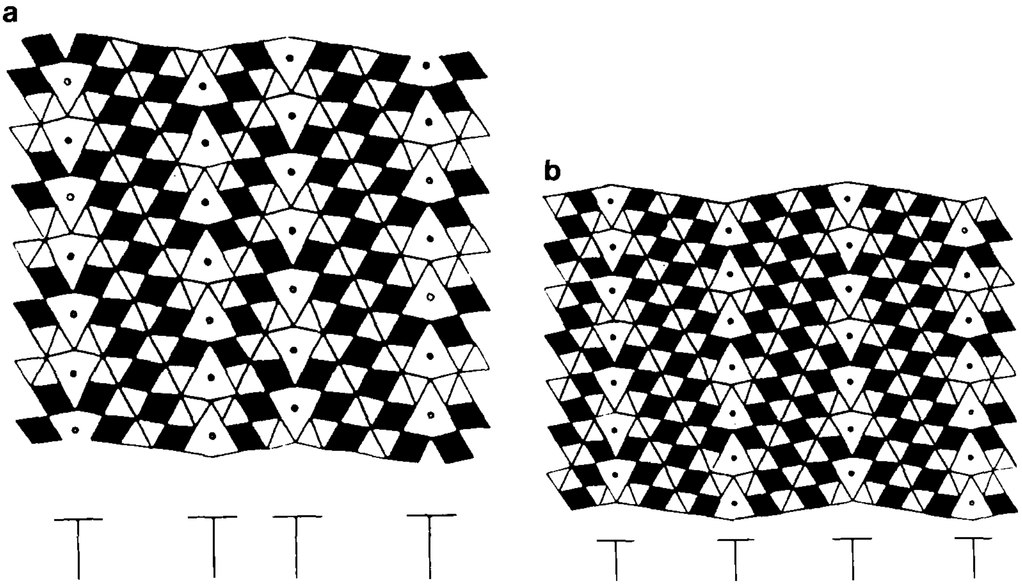

FIG. 1. The idealized structures of (a) *L*4,7 (vikingite) and (b) *L*8,8 projected down ⟨001⟩ and shown as a packing of metal–sulfur octahedra; those at a higher level are shown in light relief and those at a lower level are dark. The structures can be regarded as made up of slabs of PbS structure joined along twin planes, marked T, which contain cations in trigonal prismatic coordination.

phases with the *L*4,4 structure, lillianite, $Pb_{12}Bi_8S_{24}$, and its analog gustavite, $Pb_4Ag_4Bi_{12}S_{24}$. If the eight octahedrally coordinated Pb atoms located in the *galena*-like slabs in lillianite are substituted following the equation Ag + Bi = 2Pb, the gustavite structure is formed. The solid solution between lillianite and gustavite is accompanied by a decrease in the *b* lattice parameter as the composition changes from Ag-poor to Ag-rich (*9*, *10*).

In a previous paper the results of an electron microscope investigation into the Ag_2S–PbS–Bi_2S_3 system were reported (*1*). The studies characterized a number of new chemically twinned phases and found that for some compositions an appreciable amount of intergrowth between the twinned phases occurred. Electron microscopy, while being the best tool available for the study of disordered microstructures in nonstoichiometric materials, is, however, limited in some respects. In particular, the overall phase analysis is not convincing if only electron microscopy is used and accurate cell dimensions for the phases encountered are difficult to obtain. Thus, in parallel with the electron microscope studies, powder X-ray diffraction was used to supply these data and to characterize unit cell parameter changes with composition. We present the results of our investigations here.

Experimental

The samples studied in this investigation were prepared from elemental lead, bismuth, silver, and sulfur of "Specpure" grade supplied by Johnson Matthey Ltd. The lead, which was in the form of 7-mm-diameter rods, was cut into small fragments with a fresh scalpel after initial removal of the outer surface. The lumps of bismuth

TABLE I

LATTICE PARAMETERS OF CHEMICALLY TWINNED PHASES IN THE PBS-RICH REGION OF THE Ag_2S–PbS–Bi_2S_3 SYSTEM

Phase name	Lattice parameters (nm)				Sample	Ref.
	a	*b*	*c*	γ		
Lillianite, *L*4,4	1.3522	2.0608	0.4112		Synth.	(*8*)
	1.347	2.075	0.413		Synth.	(*6*)
	1.358	2.051	0.409		Nat.	(*18*)
	1.3535	2.0451	0.4104		Nat.	(*10*)
Vikingite, *L*4,7	1.3603(6)	2.5248(7)	0.4112(4)	95.55	Nat.	(*2, 4*)
	1.3603(6)	2.5248(7)	0.8224(8)	95.55	Nat.	(*2, 4*)
Treasurite, *L*4,8	1.3349(10)	2.6538(20)	0.4092(7)	92.77	Nat.	(*2, 4*)
Eskimoite, *L*5,9	1.3459(5)	3.0194(8)	0.4100(5)	93.35	Nat.	(*2, 4*)
Heyrovsk. *L*7,7	1.3712	3.1210	0.4131		Nat.	(*9*)
	1.3697	3.1355	0.4132		Synth.	(*8*)
	1.371	3.146	0.413		Synth.	(*6*)
	1.372	3.140	0.413			(*19*)
Ourayite, *L*11,11	1.3457(15)	4.4042(40)	0.4100(10)		Nat.	(*2, 4*)

Note. Figures in parentheses denote accuracy of the last decimal point.

were crushed into smaller fragments with a percussion mortar. Silver and sulfur were supplied as powders and were used without additional treatment.

Samples were synthesized by weighing the elements in their correct proportions and subsequently sealing the mixtures in evacuated silica tubes. The mixtures were melted at approximately 1373 K, and then cooled in three different ways: (i) brine quenched from the melt; (ii) slow cooled to 773 K, annealed at this temperature for 3 weeks, and then brine quenched; and (iii) slow cooled to 973 K, annealed at this temperature for 1 week, and then brine quenched. A list of the compositions of the samples prepared and the heat treatments each was given is contained in Table II. The compositions are also marked on the phase diagram in Fig. 2.

To determine whether phase separation had occurred in the bulk each sample was separated into different portions, all of which were X rayed. Whenever needle-like crystals formed on the surfaces of the samples these were also X rayed. The powder X-ray diffraction patterns were recorded with a Hägg–Guinier focusing camera employing strictly monochromatic Cu$K\alpha_1$ radiation. Small amounts of KCl ($a = 0.62919$ nm) were added as an internal standard. Films were measured using a scale photographed onto the film before processing to compensate for uneven film shrinkage. Unit cell dimensions were refined using least-squares methods (*11, 12*).

Results

1. Phase Analysis

Samples quenched from the melt. X-ray diffraction films of materials quenched from the melt showed rather diffuse lines, indicating that the crystalline products were disordered. This made precise phase analysis difficult, but despite this limitation *L*4,4 (lillianite) was found to be the most widely occurring twinned phase. Other phases also unmistakably identified were PbS (*galena*),

TABLE II

SAMPLE PREPARATION AND PHASE ANALYSIS

				Heat treatments						
	Composition			Initial		Final				
Sample number	PbS (mole%)	Bi_2S_3 (mole%)	Ag_2S (mole%)	Temp. (K)	Time (days)	Temp. (K)	Time (days)	Observations	X-ray diffraction analysis	Electron diffraction analysis[a]
1	85.5	14.5	—	1373	2	773	21		*L*7,7	*L*7,7
2a	85.00	12.74	2.27	1373	2	1373	2	Lines split	PbS, *L*7,7 (tr)	PbS, *L*7,7
b						773	21		PbS, *L*7,7	PbS, *L*7,7
3a	84.80	10.71	4.46	1373	2	1373	2		PbS	PbS
b						773	28		PbS	PbS
4a	79.92	19.98	0.11	1373	2	773	14		*L*7,7, *L*4,4	
b						973	14	Needl. sep.	*L*7,7	
5a	79.82	19.96	0.22	1373	2	773	14		*L*7,7, *L*4,4 (tr)	
b						973	14	Needl. sep.	*L*7,7, *L*4,4	
6a	79.72	19.93	0.35	1373	2	773	14		*L*7,7 PbS (tr)	*L*7,7 PbS
b						973	14		*L*7,7, *L*4,4	*L*4,4, *L*7,7
7a	79.60	19.90	0.50	1373	2	773	14		*L*7,7, PbS	*L*7,7 PbS
b						973	14	Needl. sep.	*L*4,4, PbS, *L*7,7	*L*4,4
8a	79.47	19.87	0.66	1373	2	773	14		*L*7,7, PbS	
b						973	14	Needl. sep.	*L*4,4, PbS, *L*4,7 (tr)	*L*4,4
9a	79.32	19.83	0.85	1373	2	773	14		*L*7,7, PbS	
b						973	14	Needl. sep.	*L*4,4, PbS, *L*7,7 (tr)	
10a	79.15	19.79	1.07	1373	2	773	14		PbS, *L*7,7 (tr)	
b						973	14		PbS, *L*7,7 (tr)	
11a	78.95	19.74	1.32	1373	2	773	14		PbS, *L*7,7 (tr)	
b						973	14	Needl. sep.	PbS, *L*4,4	
12a	78.71	19.68	1.61	1373	2	773	14		PbS	
b						973	14	Needl. sep.	PbS, *L*7,7, *L*4,4 (tr)	
13	75.0	25.0	—	1373	2	773	21		*L*4,4	*L*4,4
14a	74.94	21.05	4.01	1373	2	1373	2		PbS, *L*4,4	*L*4,4, *L*4,5
b						773	21		PbS, *L*7,7	*L*7,7
15a	75.12	17.16	7.71	1373	2	1373	2		PbS	
b						773	28		PbS, *L*7,7	
16a	74.68	14.18	11.14	1373	2	1373	2		PbS, *L*4,4 (tr), *L*7,7 (tr)	PbS, *L*4,4, *L*7,7, *L*4,5
b						773	21		PbS, *L*7,7	PbS, *L*7,7
17a	65.03	33.57	1.40	1373	2	1373	2		*L*4,4, *L*7,7 (tr)	*L*4,4, *L*7,7
b						773	21		*L*4,4	
18a	64.16	30.11	5.79	1373	2	1373	2		*L*4,4, *L*7,7	*L*4,4, *L*7,7, *L*4,7
b						773	28	*L*4,4	*L*4,4	*L*4,4
21a	58.76	39.18	2.06	1373	2	773	14		*L*4,4, GB	*L*4,4, GB
b						973	14	Needl. sep.	*L*4,4	*L*4,4
22	57.45	38.30	4.26	1373	2	773	14		*L*4,4, GB (tr)	*L*4,4, GB (tr)
23a	56.04	37.36	6.59	1373	2	773	14		*L*4,4	*L*4,4
b						973	14	Needl. sep.	*L*4,4, *L*4,7, ?	
24a	54.55	36.36	9.09	1373	2	773	14		*L*4,4	*L*4,7, *L*4,4, *L*7,7
b						973	14	Needl. sep.	*L*4,7, *L*4,4	*L*4,7, *L*4,4
25a	52.94	35.29	11.76	1373	2	773	14		*L*4,7, *L*7,7	*L*4,7, *L*7,7
b						973	14		*L*4,4, PbS, *L*4,7	
26a	51.22	34.15	14.63	1373	2	773	14		*L*8,8, PbS	*L*8,8, *L*7,8
b						973	14		*L*4,4, PbS, *L*4,7	*L*4,4, *L*4,7
27	49.37	32.91	17.72	1373	2	773	14		*L*8,8, PbS	
28	47.38	31.58	21.05	1373	2	773	14		PbS, *L*8,8 (tr)	PbS, *L*8,8
29	45.21	30.14	24.66	1373	2	773	14		PbS	
30a	54.95	43.24	1.80	1373	2	1373	2		GB, *L*4,4	GB, *L*4,4, *L*4,5
b						773	21		GB, *L*4,4, ?	GB, *L*4,4, *L*7,7
31a	54.75	38.01	7.24	1373	2	1373	2		?	*L*4,4, *L*4,5, *L*4,7, GB
b						773	28		*L*4,4, *L*4,7, ?	*L*4,4, *L*4,7, GB
32a	56.14	31.58	12.28	1373	2	1373	2		?	*L*7,7, *L*8,8, *L*4,7, *L*4,5
b						773	21		*L*7,7	*L*7,7
34	48.70	51.30	—	1373	2	973	7		GB	GB
35	47.60	32.50	19.80	1373	2	773	7		PbS, *L*8,8	PbS, *L*8,8
36a	48.60	26.20	25.20	1373	2	1373	2		PbS	PbS
b						773	21		PbS	PbS
37	47.00	38.20	14.70	1373	2	773	7		*L*8,8, ?	*L*8,8, *L*4,8, *L*4,5, *L*7,8
38	47.60	35.70	16.70	1373	2	773	7		*L*8,8, PbS	
39	35.30	44.00	20.60	1373	2	773	7		*L*8,8, PbS (tr), ?	*L*8,8, *L*4,8, *L*4,5

Note. Question marks signify that not all phases present could be identified.

[a] Reported in detail in Ref. (*1*).

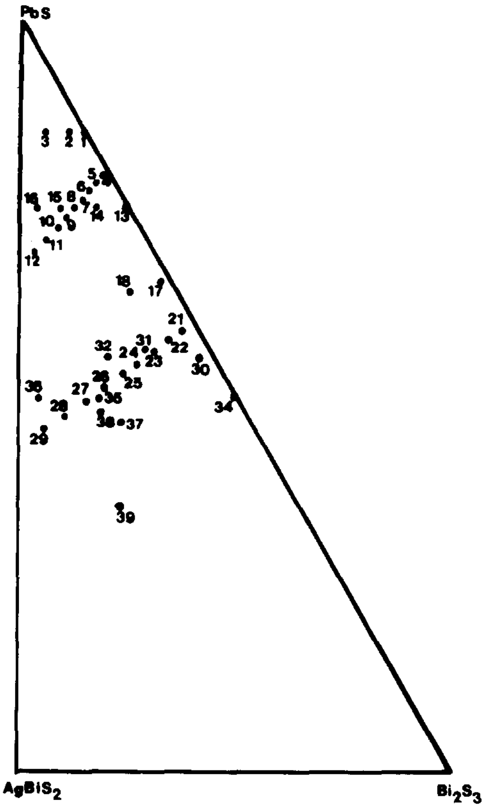

FIG. 2. Diagramatic representation of the compositions studied. The numbers correspond to the preparations detailed in Table II.

*L*7,7 (heyrovskyite), and galenobismuthite, which is not a member of the lillianite series. In the region of samples 31 and 32 it was not possible to determine which phases were present due to the very diffuse nature of the lines. The results of the phase analysis at this temperature are shown schematically in Fig. 3a.

Samples annealed at 973 K. In these preparations a considerable separation of phases occurred within the silica tubes. Needle-like crystals frequently grew from the bulk during annealing. Most often they were *L*4,4 (lillianite), although *L*4,7 (vikingite) was also found to separate in this way. In the bulk, *L*4,4 (lillianite) was found to coexist with other phases over a wide range of compositions. Within the series of samples 21–29 five phases could be recognized: galenobismuthite, *L*4,4 (lillianite), *L*4,7 (vikingite), *L*8,8, and *galena*. *L*4,7, (vikingite), was found to predominate in only one sample and occurred in three others in traces. *Galena* coexisted with *L*7,7 (heyrovskyite) for PbS-rich samples and with *L*8,8 for PbS-poor compositions. The lattice parameter of the *galena* phase decreased slightly as the overall composition of the samples became richer in *L*7,7 or *L*8,8. The results of the phase analysis at this temperature are summarized in Fig. 3b.

Samples annealed at 773 K. In these preparations *L*7,7 (heyrovskyite) and *galena* occurred in the region close to PbS, while in the series of samples 21–29, four other phases, galenobismuthite, *L*4,4 (lillianite), *L*4,7 (vikingite), and *L*8,8, could be identified. X-ray films from samples 37 and 39 could not be fully interpreted as the lines were too diffuse, but it is possible to say that the *L*8,8 phase was present, together with a phase or phases that could not be identified. X-ray films from samples 24, 25, and 32 that lie in the center of the phase region also had very diffuse lines. Special attention was paid to the X-ray diffraction patterns of samples 26–29 and 35–39 in search for *L*5,9 (eskimoite), which has been reported to occur near the composition straddled by these preparations, but no trace of this phase was found. The results of the phase analysis at this temperature are summarized in Fig. 3c.

2. *Lattice Dimensions*

L4,4 (lillianite). Silver free synthetic lillianite, $Pb_{12}Bi_8S_{24}$, that was annealed at 773 K for 3 weeks was initially studied to provide a comparison with materials containing silver. The X-ray diffraction patterns were refined to give an orthorhombic unit cell with dimensions $a = 1.3540(4)$ nm, $b = 2.0654(4)$ nm, $c = 0.4111(1)$ nm.

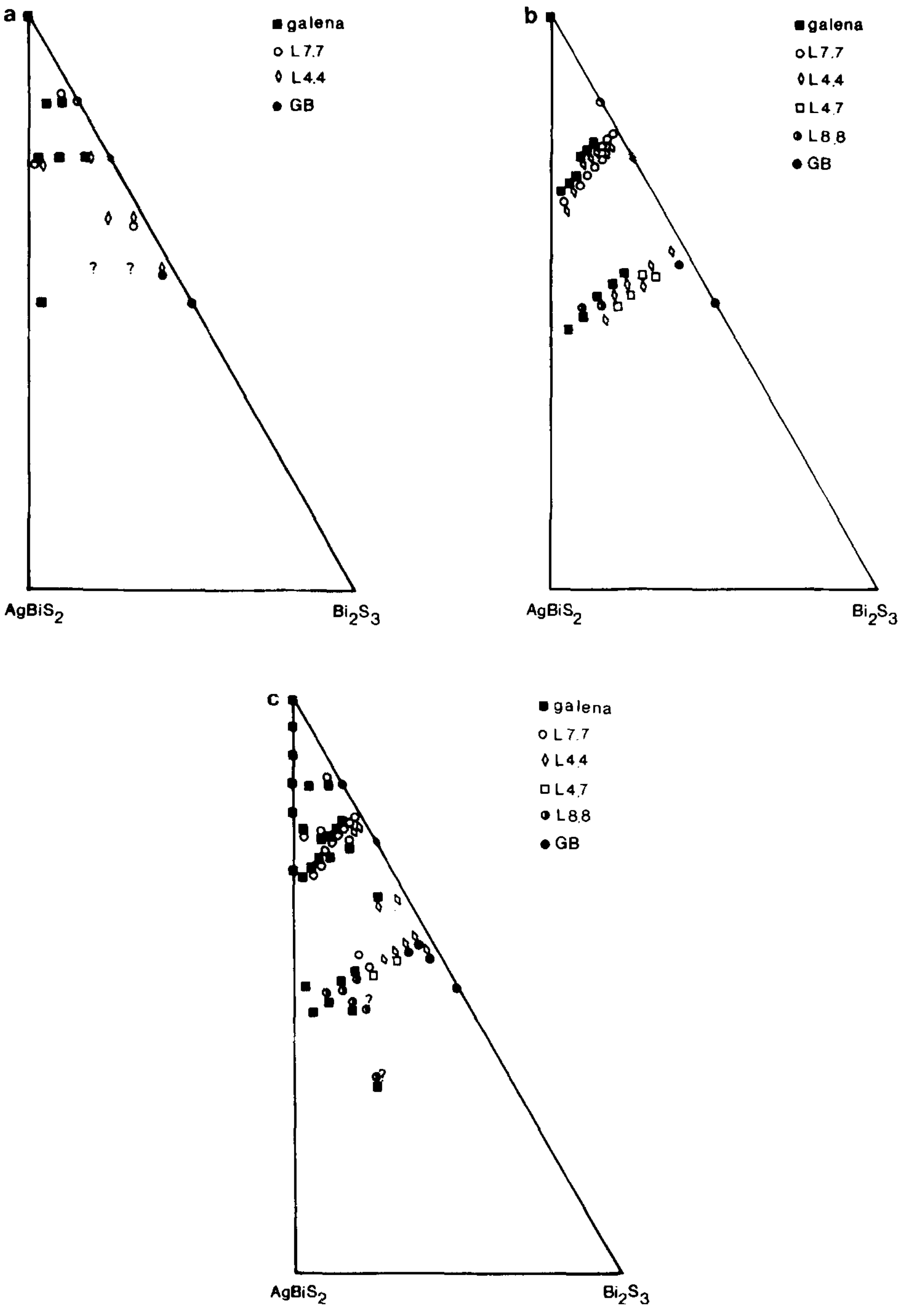

FIG. 3. Diagramatic representation of the results of powder X-ray phase analysis of samples (a) quenched from the melt, (b) annealed at 973 K, and (c) annealed at 773 K. GB denotes galenobismuthite. Question marks signify that not all phases present could be identified.

TABLE III

LATTICE PARAMETER DATA FOR CHEMICALLY TWINNED PHASES FOUND IN THIS STUDY

Phase name	Sample number	Temp (K)	Lattice parameters (nm)			
			a	*b*	*c*	γ
Lillianite	13	773	1.3540(4)	2.0654(4)	0.4111(1)	
Lillt-gust. s.s.	21	773	1.3499(4)	2.0545(4)	0.4123(1)	
Lillt-gust. s.s.	17	773	1.3511(4)	2.0499(4)	0.4114(1)	
Lillt-gust. s.s.	31	773	1.3462(4)	2.0397(6)	0.4098(2)	
Lillt-gust. s.s.	23	973	1.3480(4)	2.0312(5)	0.4117(1)	
Lillt-gust. s.s.	22	773	1.3471(2)	2.0304(4)	0.4112(1)	
Lillt-gust. s.s.	23	773	1.3478(4)	2.0255(4)	0.4101(1)	
Vikingite	24	973	1.3461(3)	2.5664(4)	0.4105(1)	95.57(2)
Viking. s.s.	23	973	1.3514(9)	2.5590(1)	0.4102(3)	95.59(5)
Heyrovskyite	1	773	1.4670(9)	3.1368(6)	0.4143(1)	
Heyrovsk. s.s.	7	773	1.4621(2)	3.1081(6)	0.4133(1)	
Heyrovsk. s.s.	8	773	1.3623(2)	3.1000(4)	0.4119(1)	
Heyrovsk. s.s.	32	773	1.3494(4)	3.0679(5)	0.4105(1)	
*L*8,8	26	773	1.3565(4)	3.3046(7)	0.4102(2)	

Note. Figures in parentheses denote accuracy of the last decimal point; s.s. stands for solid solution.

The lattice parameters of a number of samples with the *L*4,4 structure which were taken from preparations containing Ag were refined. The results are presented in Table III. It is seen that the value of the *a* dimension decreased slightly and the *b* dimension decreased appreciably in the Ag-containing samples, while the *c* parameter remained almost unchanged. There were no apparent changes in the relative intensities of reflections as the composition changed from lillianite toward gustavite.

L4,7 (*vikingite*). Although this phase has been found in mineral samples (*2, 4*) this is the first report of synthetic vikingite, *L*4,7. X-ray diffraction data were refined to give a monoclinic unit cell with dimensions a = 1.3461(3) nm, b = 2.5664(4) nm, c = 0.4105(1) nm, γ = 95.57°. The two space groups allowed by the systematic extinctions found, which were h, k, l: $h + l = 2n$; h, k, l: $h = 2n$, and $00l$: $l = 2n$, are *B*2/*m* and *Bm*. Within the compositions investigated it appears that the *L*4,7 structure persists only over a narrow phase range and only small changes of the lattice parameters were observed. Two values are given in Table III to illustrate this.

L7,7 (*heyrovskyite*). The X-ray data of silver free heyrovskyite, $Pb_{24}Bi_8S_{36}$, showed the unit cell to be orthorhombic with dimensions a = 1.367(9) nm, b = 3.1368(6) nm, c = 0.4143(1) nm, in good agreement with that reported by Otto and Strunz (*2*). Incorporation of silver into the structure caused a similar change in the cell dimensions to that observed for *L*4,4 (lillianite), with the *b* parameter decreasing noticeably as the silver content increased and the *a* parameter decreasing slightly. The details are presented in Table III.

L8,8. The X-ray data for this new twinned phase yielded a refined unit cell which was orthorhombic with dimensions a = 1.3565(4) nm, b = 3.3046(7) nm, c = 0.4102(2) nm. The space group allowed by the systematic extinctions is *Bbmm*. The phase did not occur in sufficient samples for the variation of cell dimensions with Ag content to be assessed.

Discussion

The data summarized in Fig. 3 indicate that *L*4,4 (lillianite) is the most stable phase at elevated temperatures for PbS-rich compositions. This feature may be connected with the fact that this material has the narrowest *galena*-like slabs of all the twinned phases so far found in the lillianite–galenobismuthite–gustavite compositional triangle. The phases with wider *galena*-like slabs, such as *L*7,7 (heyrovskyite) and *L*8,8 were found at lower temperatures. This suggests that the phases ourayite, *L*11,11, and eskimoite, *L*5,9, which are known from mineral samples, were not found in this study because the temperatures used in the syntheses were too high. Experiments in which samples are annealed at temperatures below 773 K are planned to see if these structures will form under these conditions.

Although after annealing the majority of samples gave sharp X-ray powder patterns, preparations in the region of samples 24, 25, and 32 consistently gave X-ray diffractograms which could not be fully interpreted due to the diffuse nature of the lines. This region of disorder corresponds to a postulated "mosaic" phase, called *schimerite* reported by Makovicky and Karup-Møller (*8*). The nature of the disorder that occurred in this phase region was revealed by high-resolution electron microscope studies (*5*). It was found that the twinned phases which occur in this phase region, especially *L*4,4 and *L*4,7, had a tendency to form disordered or sometimes partially ordered intergrowths. In view of the electron microscope results we suggested that schimerite can be defined as an intergrowth of phases rather than a single phase.

The results of the unit cell refinements show that only the *b* parameters of the unit cells of the twinned phases change significantly as silver is incorporated into the crystal structure. The observation raises two points: why does the structure shrink with the substitution and why does only one lattice parameter decrease significantly?

The first point can be explained in terms of the interatomic distances normally found in related sulfides. If the following values of metal–sulfur distances in octahedral coordination are taken, S–Ag^{1+} = 0.2782 nm, S–Bi^{3+} = 0.2826 nm, and S–Pb^{2+} = 0.2948 nm (*13*), one can see that substitution of Pb for Bi or Ag results in a contraction of an *M*–S bond, which is sufficient to account for the cell parameter changes observed. The second point is explained if the substitution takes place in the *galena*-like slabs leaving the dimensions of the trigonal prismatic twin planes unchanged. In order to ensure that only the parameter *b* of the structure changes, while *a* stays almost constant, the metal–sulfur octahedra that build the slabs have to distort mainly in the ⟨111⟩ direction of the PbS substructure. Such a distortion is reasonable as calculations show this would cause the minimum increase in elastic strain energy (*14*). Thus the structures of silver bearing twinned phases can be envisaged as possessing a skeleton of relatively fixed trigonal prisms occupied by lead cations which are connected by flexibly wide, *galena*-like slabs which contain Pb, Bi, and Ag cations.

Despite the substantial data concerning compositions of silver containing natural lillianites, little is known at present about the relationship between the degree of Ag substitution and unit cell dimensions, as complete X-ray data is only available for minerals with compositions close to the end members of the lillianite–gustavite join (*9*). In the only study of synthetic materials reported to date, by Hoda and Chang (*10*), the true compositions of the substituted lillianites were not known. A comparison of the results show that the *b* parameters of the synthetic materials are appreciably bigger than those of the corresponding minerals. Our results seem to support Hoda and Chang's findings, indicating that other factors in addition to silver substitution are of importance in natural specimens.

The incorporation of silver into the PbS–Bi_2S_3 system not only changes the lattice parameters of the twinned phases but also stabilizes new structures. For example, the phase $L4,7$ forms in the presence of silver but not in its absence even though both $L7,7$ and $L4,4$ are stable in the PbS–Bi_2S_3 system. To investigate whether silver was incorporated into the *galena*-like slabs of the $L4,7$ structure to stabilize the phase we can turn to the lattice parameter data presented above. As the lattice parameter refinement shows, the separation of the twin planes that delineate the unit cell of $L4,7$ is $2.5661 \times \cos(\gamma - 90) = 2.552$ nm. If we assume that there is no silver in the structure then the separation should be very near to half of the value obtained by adding the twin plane separation of silver free $L4,4$ and $L7,7$, which gives a value of 2.601 nm. The experimentally measured distance in $L4,7$ is smaller than this latter value, confirming that silver was incorporated into the structure to stabilize it. Because the amount of silver needed to stabilize this structure is likely to be fairly precise, a wide composition range is not to be expected for this structure.

Although this and the preceding paper (*1*) have succeeded in clarifying structural relations in the Ag_2S–PbS–Bi_2S_3 system, a number of problems remain. A low-temperature study would be of great interest in the search for phases with *galena*-like slabs wider than eight octahedra. Additionally, microanalysis of individual crystal fragments via electron microscopy would be very helpful in shedding some light on the problem of silver and bismuth distribution within the *galena*-like regions, a result needed to understand the stability of monoclinic twinned phases.

Acknowledgments

A.S. is indebted to the British Council and I.C.I. plc. for financial support.

References

1. S. Andersson and B. G. Hyde, *J. Solid State Chem.* **9,** 92 (1974).
2. H. H. Otto and H. Strunz, *Neues Jahrb. Mineral Abh.* **108,** 1 (1968).
3. Y. Takéuchi and J. Takagi, *Proc. Japan Acad.* **50,** 76 (1974).
4. J. Tagaki and Y. Takéuchi, *Acta Crystallogr. Sect. B* **28,** 649 (1972).
5. A. Skowron and R. J. D. Tilley, submitted for publication.
6. S. Karup-Møller, *Bull. Geol. Soc. Denmark* **26,** 41 (1977).
7. E. Makovicky and S. Karup-Møller, *Neues Jahrb. Mineral. Abh.* **130,** 264 (1977).
8. E. Makovicky and S. Karup-Møller, *Neues Jahrb. Mineral. Abh.* **131,** 56 (1977).
9. E. Makovicky and S. Karup-Møller, *Neues Jahrb. Mineral. Abh.* **131,** 264 (1977).
10. S. N. Hoda and L. L. Y. Chang, *Amer. Mineral.* **60,** 621 (1975).
11. A. G. Nord, *Inorg. Phys. Chem.* **33,** 42 (1963).
12. P. E. Werner, *Ark. Kemi* **31,** 513 (1969).
13. D. Altermatt and I. D. Brown, *Acta Crystallogr. Sect. B* **41,** 240 (1982).
14. G. N. Ramachendran and W. A. Wooster, *Acta Crystallogr.* **4,** 431 (1951).